A Dynamical System Based Approach for Controlling Robotic Manipulators During Non-contact/Contact Transitions

Seyed Sina Mirrazavi Salehian* and Aude Billard

***Abstract*— Many daily life tasks require precise control when making contact with surfaces. Ensuring a smooth transition from free motion to contact is crucial as incurring a large impact force may lead to unstable contact with the robot bouncing on the surface, i.e. chattering. Stabilizing the forces at contact is not possible as the impact lasts less than a millisecond, leaving no time for the robot to react to the impact force. We present a strategy in which the robot adapts its dynamic before entering into contact. The speed is modulated so as to align with the surface. We leverage the properties of autonomous dynamical systems for immediate re-planning and handling unforeseen perturbations and exploit local modulations of the dynamics to control for the smooth transitions at contact. We show theoretically and empirically that by using the modulation framework, the robot can (I) stably touch the contact surface, even when the surface's location is uncertain, (II) at a desired location, and finally (III) leave the surface or stop on the surface at a desired point.**

I. Introduction

Establishing a stable contact with an environment is the first step toward accomplishing interactive tasks. A wide variety of many real-world manipulation tasks, such as milling/polishing/finishing workpieces [1], [2], wiping/painting surfaces [3], [4], peeling or dough rolling [5], include interactions between a tool and an environment. For such applications, the complete scenario can be categorized into three *regions*: (I) Moving in *free motion* space and approaching the contact surface; i.e. *Free motion* region. (II) Establishing the contact with the surface; i.e. *Transition* region. (III) Maintaining the contact with the surface while moving in the other directions; i.e. *Contact* region.; see Fig.1. In this paper, *we call a contact stable if the impact happens only once and the robot remains in contact with the surface after the impact.*

Achieving a stable contact is particularly challenging as the contact leaves an infinitesimally short window of time for the robot to react properly to the impact force. It is however necessary to control for stable contact to avoid that the robot bouncing on the surface and damaging itself or the environment. Importantly, the complexity of the environment increases if the arm and the surface do not dissipate impact energy, i.e., perfectly elastic impact. In this case, to successfully establish a contact with a rigid surface, the robot should touch the surface with zero velocity so that the post-contact velocity taken along the line of impact is zero. Nevertheless, impacts in real-world scenarios are mainly inelastic, where,

All authors are with the School of Engineering, Ecole Polytechnique Federale de Lausanne (EPFL), Switzerland. {sina.mirrazavi;aude.billard}@epfl.ch

*Corresponding author.

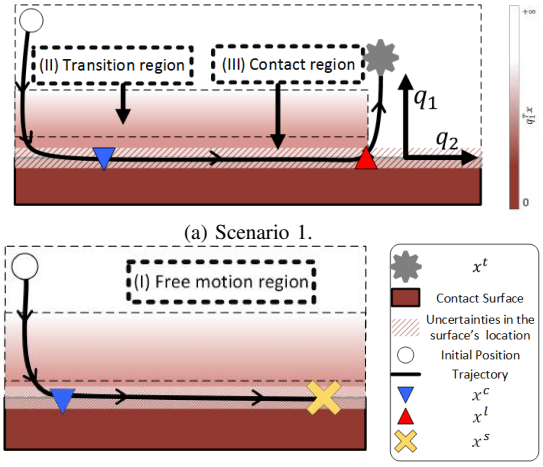

(a) Scenario 1.

(b) Scenario 2.

Fig. 1: Schematic of three subtasks of an interactive application while the surface's location is uncertain. The arm starts approaching the surface at the *free motion* region. Once it is close enough to the surface, it regulates its velocity to establish a stable contact at the desired contact point (x^c). Then while sliding on the surface, based on the scenario requirements, it either leaves the surface (Fig.1a) or reaches the target on the surface (Fig.1b) at desired departure (x^l) or stop (x^s) locations, respectively. $q_i \; \forall i \in \{1,2\}$ form an orthogonal bases in $\mathbb{R}^2$.

if the robot does not pass through the contact surface or the impact does not release energy, the relative post-contact velocity is a fraction of the relative pre-contact velocity [6]. In this case, touching the surface with near-to-zero velocity results in a zero post-contact velocity along the impact line, i.e., the robot remains in contact with the surface after the impact [7].

The complexity of achieving a stable contact has attracted attention in the last two decades. Early approaches addressed the stable contact problem with position/force hybrid control architectures. [8]–[11] proposed a hybrid control architecture in which a stable contact can be ultimately established after a finite number of bounces. On the same track, [7], [12] proposed three control laws for the three motion regions. Once the first impact has occurred, the controller at the *transition* region is activated which, asymptotically, reduces the normal velocity to zero. In [13], an integral force compensation with a velocity feedback controller is proposed for force tracking and rejecting the effect of impacts, where the force regulation is activated as soon as the force sensor detects the impact. Indirect force control architectures address the problem of switching between controllers [14]. [15] proposed a two layers controller which consists of an impedance and an admittance controllers. The parameters of the latter are calculated by solving a Linear Quadratic Regulator problem to minimize the force overshooting. In [16], [17],

a hybrid impedance(admittance)/time-delayed controller is proposed to absorb the impact force where the control input becomes zero if the contact force is not sensed. By artificially saturating the feedback sensors and modeling the contact surface via a passive mass-spring system, a controller for a 2-DOF planar robotic arm is proposed to limit the impact force in [18]. [19] shows that the classical PD feedback control law can be effectively used for mechanical systems subject to inequality constraints. By assuming the contact surface is a passive mass-spring system, [20] developed an adaptive control architecture to push the system to a desired state while the dynamics of neither the robot nor the environment are precisely known. The proposed controller in [21] guarantees stabilization of the manipulator on the contact surface after a finite number of bounces. By applying the concept of energy tanks, [4], [22] proposed tank-based approaches to ensure the stability of robotic arms driven by variable impedance controllers during non-contact/contact transitions. Even though in the mentioned works, it can be proved that the robot's motion is stable and the contact is asymptotically/ultimately stable, there is no guarantee that the robot does not bounce on the surface after the first impact.

By approximating the contact surface with a passive spring system and dividing the state space into five regions, [23] uses the feedback force to propose piecewise affine controllers for each region such that a stable impact is achieved for linear one dimensional systems. However, in [23] the stable impact is achieved if the environment and the tool can be precisely modeled via a spring system and the bandwidth of the position and force sensors and the communication delays are infinite and zero, respectively.

In this paper, we exploit the properties of Dynamical Systems (DS) for immediate re-planning and their inherent robustness to real-time perturbations and propose an actively compliant control strategy. In [24] and later in [25] and [28] , we propose dynamical systems to intercept a moving object with zero relative velocity by a single or a multi-arm system, respectively. Those proposed DSs are particularly tailored for the reaching and softly intercepting moving objects. In this work, as the *transition* is a local behavior, we propose a strategy consisting of locally modulating the robot's motion in such a way that a stable contact can be established, even when the location of the contact surface is uncertain. The proposed architecture can be integrated into existing DS-based motion control approaches and modulates the robot's motion in dynamic scenarios, where the robot must adapt to fast external perturbations. The idea of locally modulating dynamical systems is not novel and it has been previously used in [26] and [27] for modulating first order DSs. In this contribution, we use this idea to modulate the motion of a robot such that:

Objective 1 : If the robot contacts the surface, the impact happens only once and the robot remains in contact after the impact.

Moreover, we show that the proposed controller is capable of modulating the robot's motion such that:

Objective 2 : The robot contacts the surface at a specific point (x^c).

Objective 3 : If the robot is in contact with the surface, it slides on the surface and either

a) leaves the surface at a specific departure location (x^l), see Fig.1a, or

b) stops at a specific stop location (x^s) on the surface, see Fig.1b.

As the main scope of this paper is the stability of contact and not the closed-loop motion generator, we have assumed that the robot is able to exactly follow the generated motion at the position level. The rest of the paper is organized as follows. We formalize our assumptions and problem formulation in Section II. Section III develops our controller. The approach's performance is evaluated on real world robot experiments in Section IV. This paper concludes with a discussion of the limitations and future extensions in Section V.

II. Problem Statement

Suppose the contact surface is non-penetrable, passive and flat. Moreover, a continuous function ($\Gamma(x) = {q_1}^T x$), which conveys a notion of distance to the surface is available, where N is the unit normal vector to the surface and x denotes the position of the robot's end-effector. By definition, the origin of the coordinate frame is on the surface and the surface corresponds to the plane ${q_1}^T x = 0$. Based on this definition, one can categorize the task space into two regions: the *free motion* region when $0 < {q_1}^T x$ and the *contact* region when ${q_1}^T x = 0$.

We consider the following continuous-time system. As the aim of this paper is controlling both position and velocity at the contact, the DS must be a function of both of them and the output must define the desired acceleration of the robot.

$$\ddot{x} = \mathsf{M}(x,\dot{x}) f(x,\dot{x},t) \tag{1}$$

where $f(x,\dot{x},t)$ represents the nominal dynamical system which generates the nominal arm behavior. We assume that the nominal DS is asymptotically stable to a fixed target (x^t) located above the surface, i.e., $0 < {q_1}^T x^t$.[1] Furthermore, the nominal acceleration is non-zero everywhere except on the target; i.e. $f^T(x,\dot{x}) f(x,\dot{x}) \neq 0 \ \forall (x,\dot{x}) = \mathbb{R}^{d\times d} - \{x^t, 0\}$.[2] $\mathsf{M}(x,\dot{x}) \in \mathbb{R}^{d\times d}$ is a modulation function which reshapes the nominal DS such that it complies with the contact surface based on the state of the robot. We define the modulation function as follows:

$$\mathsf{M}(x,\dot{x}) = Q\Lambda Q^T \quad Q = \begin{bmatrix} q_1 & \dots & q_d \end{bmatrix} \tag{2}$$

where $q_i \ \forall i \in \{1,\dots,d\}$ form an orthonormal basis in $\mathbb{R}^d$ as shown in Fig.1a. $\boldsymbol{\lambda}_{ij}(x,\dot{x}) \ \forall i,j \in \{1,\dots,d\}$ are the

[1] It is important to note that asymptotically stability of the nominal DS is only required to achieve *Objective 3*.a. To achieve the other objectives(*Objective 1*, *Objective 2* and *Objective 3*.b) it is not necessary for the nominal DS to be stable.

[2] If $M(x,\dot{x})$ is the control input, this assumption is equivalent to the controllability of $\ddot{x} = \mathsf{M}(x,\dot{x}) f(x,\dot{x},t)$.

entries of Λ, where i is the row number and j is the column number. The motion direction, tangential and normal to the surface, can be controlled through the scalar values $\boldsymbol{\lambda}_{ij}\ \forall i,j \in \{1,\dots,d\}$. As an example, by setting $\boldsymbol{\lambda}_{1j}(x,\dot{x}) = 0\ \forall j \in \{1,\dots,d\}$, the acceleration of the robot normal to the surface will be zero; i.e. ${q_1}^T\ddot{x} = 0$. Moreover, by setting $\boldsymbol{\lambda}_{ii}(x,\dot{x}) = 1,\ \boldsymbol{\lambda}_{ij}(x,\dot{x}) = 0\ \forall i,j \in \{1,\dots,d\},\ i \neq j$, the nominal DS drives the robot in the q_i^{th} direction. We exploit this property and limit the influence of the modulation function to a region in a vicinity of the surface; denoted as the *transition* region.[3]. Given that we have at our disposal the function $\Gamma(x)$ to measure the distance to the surface, we set the *transition* region to be all points such that $0 < \Gamma(x) \leq \rho,\ \rho \in \mathbb{R}_{>0}$. Outside this region, to avoid undesirable modulations, the modulation exponentially decreases as a function of the distance to the surface. To modulate locally the dynamics of the DS given by (1) and (2), we set:

$$\boldsymbol{\lambda}_{ij}(x,\dot{x}) = \begin{cases} \lambda_{ij}(x,\dot{x}) & \text{if } \Gamma(x) \leq \rho \\ (\lambda_{ij}(x,\dot{x}) - 1)\, e^{\frac{\rho - \Gamma(x)}{\sigma}} + 1 & \text{if } i = j\ \rho < \Gamma(x) \\ \lambda_{ij}(x,\dot{x}) e^{\frac{\rho - \Gamma(x)}{\sigma}} & \text{if } i \neq j\ \rho < \Gamma(x) \end{cases} \tag{3}$$

$\forall i,j \in \{1,\dots,d\}$ where $0 < \sigma$ defines the speed at which the modulation vanishes in the free motion region. ρ defines the region of the influence of the modulation function. If $\rho < \Gamma(x)$, the robot is far from the contact surface and $\Lambda = I_{d\times d}$; i.e. the robot is driven solely by the nominal dynamical system.

In the following section, we show how by defining $\lambda_{ij}\ \forall i,j \in \{1,\dots,d\}$, a stable contact can be achieved. Moreover, we define ρ based on the kinematic constraints of the robot. First, we consider a perfect elastic impact between the robot and the contact surface; i.e. the Coefficient Of Restitution (COR)[4] (e) is one. Then, we extend this to a realistic scenario where the impact is inelastic, i.e. $0 \leq e < 1$.

III. Compliant Modulation Function

A. The elastic impact

Consider a scenario where the impact is perfectly elastic $(e = 1)$. In this case, the normal velocities[5] of the robot before and after the impact are equal in amplitudes but pointing to opposite directions. Hence, to achieve a stable contact (*Objective 1*), the normal velocity of the robot at the contact must be zero, i.e., ${q_1}^T\dot{x}(t^*) = 0$, where, t^* is the time when the robot enters into the contact with the surface.

Theorem 1: For a given initial state $\{x_0, \dot{x}_0 \in \mathbb{R}^d |\ 0 < {q_1}^T x_0 \leq \rho, f(x_0,\ \dot{x}_0) \neq 0\}$, the motion generated by (1) and (2) makes contact with the surface with zero normal velocity and satisfies *Objective 1*, if $\forall j \in \{1,\dots,d\}$

$$\lambda_{1j}(x,\dot{x}) = \left(-2\omega N^T\dot{x} - \omega^2 N^T x\right)\mathbf{f}_j(x,\dot{x},t) \tag{4}$$

[3]The development of the *transition* region is partly inspired from the potential field obstacle avoidance approaches [29].

[4]COR is defined as the ratio of velocities after and before an impact, taken along the line of the impact.

[5]For sake of simplicity, in the rest of the paper, we call the velocity normal to the surface, the normal velocity.

where $\mathbf{f}_j(x,\dot{x},t) = \frac{f(x,\dot{x},t)^T q_j}{f(x,\dot{x},t)^T f(x,\dot{x},t)}$ and

$$\frac{|{q_1}^T\dot{x}_0|}{{q_1}^T x_0} \leq \omega \tag{5}$$

Moreover, the motion generated by (1) and (2) makes contact with the surface at x^c and satisfies *Objective 2*, if $\forall (i,j) \in \{(2,1),(2,2),\dots,(d,d)\}$

$$\lambda_{ij}(x,\dot{x}) = \left(-2\omega {q_i}^T\dot{x} - \omega^2 {q_i}^T(x - x^*)\right)\mathbf{f}_j(x,\dot{x}) \tag{6}$$

Where $x^* = x^c$.

Proof: see Appendix A.

Theorem 1 provides a function to modulate the motion of the robot's end-effector such that stable contact can be established at the desired location. However, it is important to note that defining the pre-specified contact location is not necessary for implementing the proposed modulation framework. For instance, by defining

$$\lambda_{ij}(x,\dot{x}) = \begin{cases} 0 & \text{if } i \neq j \\ 1 & \text{if } i = j \end{cases} \quad \forall i \in \{2,\dots,d\} \quad \forall j \in \{1,\dots,d\} \tag{7}$$

and $\lambda_{1j}(x,\dot{x}),\ \forall j \in \{1,\dots,d\}$ by (4), the motion of the nominal DS is modulated only in the normal direction. Hence, if the robot enters the transition region, it stably makes contact with the surface as the normal velocity of the robot is modulated based on (4). However, the contact location emerges from the motion generated by the nominal DS.

If the robot starts its motion outside of the transition region, Eq. (3) states that the modulation function is activated once it enters the region. Hence, the initial state $({q_1}^T x_0)$ in Theorem 1 is equivalent to ρ. However, Theorem 1 depends on the dynamics of the robot and is achievable only if the robot can decelerate sufficiently fast. Hence, the transition region must be set sufficiently large to meet the robot's physical limits. This is summarized in the following proposition:

Proposition 1: For a robot with upper bounds $\dot{x}_{max}$ and $\ddot{x}_{max}$ on velocity and acceleration, respectively, given ${q_1}^T x_0 = \rho$, we set ρ and ω in (3) and (4), respectively, such that $\rho = \frac{3({q_1}^T\dot{x}_{max})^2}{|{q_1}^T\ddot{x}_{max}|},\ \omega = |\frac{{q_1}^T\ddot{x}_{max}}{3{q_1}^T\dot{x}_{max}}|$.

Proof: see Appendix B.

Once the robot is in *contact* with the surface, two interactive scenarios can be accomplished. In the first scenario, the robot slides on the surface and leaves it at the specific departure location (x^l); see Fig.1a. In the second scenario, the robot slides on the surface till it reaches the desired stop location on the surfaces (x^s); see Fig.1b. The former can be achieved by modulating the nominal dynamical system, x^* and the definition of $\Gamma(x)$. Whereas, the latter can be achieved by modulating only the nominal DS and x^*. These are summarized in the following propositions:

Proposition 2: For a given initial state $\{x_0, \dot{x}_0 \in \mathbb{R}^d |\ {q_1}^T x_0 \leq \rho, f(x_0,\ \dot{x}_0) \neq 0\}$, the motion generated by the nominal DS (1) modulated by (2), where

$\lambda_{ij}(x,\dot{x}),\ \ \forall(i,j) \in \{(1,1),(1,2),\ldots,(d,d)\}$ are defined by (4) and (6), makes contact with the surface at x^c and then slides on the surface till it asymptotically reaches x^s (i.e. satisfaction of *Objective 3*.b) if x^* in (6) is such that:

$$x^* = \begin{cases} x^c & \text{if } 0 < {q_1}^T x \\ x^s & \text{if } {q_1}^T x = 0 \end{cases} \tag{8}$$

Where, x^s is defined on the surface.

Proof is omitted as it is similar to the one given in Appendix A.

***Proposition** 3:* For a given initial state $\{x_0, \dot{x}_0 \in \mathbb{R}^d |\ {q_1}^T x_0 \leq \rho, f(x_0,\ \dot{x}_0) \neq 0\}$, the motion generated by the nominal DS (1) modulated by (2), where $\lambda_{ij}(x,\dot{x}),\ \ \forall(i,j) \in \{(1,1),(1,2),\ldots,(d,d)\}$ are defined by (4) and (6), makes contact with the surface at x^c and then leaves it at x^l (i.e. satisfaction of *Objective 3*.a) if x^* and $\Gamma(x)$ in (6) and (3), respectively, are defined as follows:

$$x^* = \begin{cases} x^c & \text{if } 0 < {q_1}^T x \\ 2x^l - x^c & \text{if } {q_1}^T x = 0 \end{cases} \tag{9}$$

$$\Gamma(x) = {q_1}^T x + \left(\rho - (x^l - x^c)^T (x^l - x)\right) e^{-(x^l-x)^T \Sigma^{-1} (x^l - x)} \tag{10}$$

Where, x^l is defined on the surface and $\Sigma \in \mathbb{R}^{d\times d}$ is a positive definite matrix.

Proof: see Appendix C.

As (4) is not a function of x^*, changing x^* does not influence the motion of the robot in the normal direction to the surface. Σ defines the influence of $\left(\rho - (x^l - x^c)^T (x^l - x)\right) e^{-(x^l-x)^T \Sigma^{-1} (x^l - x)}$ over ${q_1}^T x$ in (10). If all entries in Σ are small, its influence will be small and vice-versa.

B. The inelastic impact

In an inelastic impact, due to internal friction, kinetic energy is dissipated and hence the coefficient of restitution is less than one, i.e., $0 \leq e < 1$. In this case, we can assume that if the normal velocity of the robot is very small ($-1 \ll \delta_{\dot{x}} \leq 0$) on contact, the surface absorbs all the kinetic energy of the arm, i.e. the end-effector remains in contact after the impact[6]. Hence, to achieve *Objective 1*, the velocity of the robot must satisfy the following constraint at impact:

$$\delta_{\dot{x}} \leq {q_1}^T \dot{x}(t^*) \leq 0 \tag{11}$$

***Theorem** 2:* Assuming the impact is inelastic. For a given initial state $\{x_0, \dot{x}_0 \in \mathbb{R}^d |\ 0 < {q_1}^T x_0 \leq \rho,\ \ f(x_0,\dot{x}_0) \neq 0\}$, the dynamical system (1) and (2) satisfies condition (11), if $\lambda_{1j}(x,\dot{x}) =$

$$\begin{cases} \omega\left(-{q_1}^T \dot{x} + (\delta_{\dot{x}} + \nu)\right) \mathbf{f}_j(x,\dot{x}) & {q_1}^T \dot{x} < \delta_{\dot{x}} \quad (12) \\ \omega\left(\dfrac{\nu}{\delta_{\dot{x}}} {q_1}^T \dot{x} - \omega(1 - \dfrac{{q_1}^T \dot{x}}{\delta_{\dot{x}}}) {q_1}^T x\right) \mathbf{f}_j(x,\dot{x}) & \delta_{\dot{x}} \leq {q_1}^T \dot{x} \leq 0 \quad (13) \\ \omega\left(-2N^T \dot{x} - \omega N^T x\right) \mathbf{f}_j(x,\dot{x}) & 0 < {q_1}^T \dot{x} \quad (14) \end{cases}$$

[6]This assumption is adopted from [7].

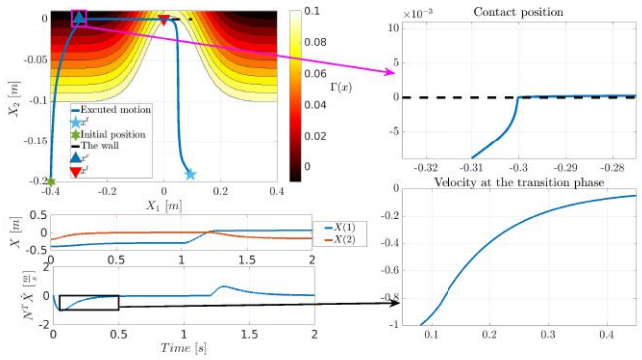

(a) Stable contact is achieved by using the proposed modulation function. $\Gamma(x)$ is defined based on (10). The contact is assumed inelastic. $\rho = 0.1$, $\sigma = 0.01$, $\omega = 0.1$, $\nu = 0.01$ and $\delta_{\dot{x}} = -0.02$. As it is illustrated above, at the *transition* region, the velocity of the robot is reduced based on Theorem 2 such that it satisfies (11). Moreover, in the tangential directions, the robot regulates its velocity based on (6) and touches the surface exactly at the desired contact point ($x^c = [-0.3\ \ 0]^T$). As it is shown in this example, based on Proposition 3, the robot leaves the surface at the desired leaving point ($x^l = [0\ \ 0]^T$) .

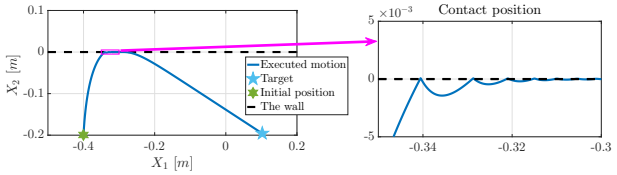

(b) The modulation function is disabled by setting $M = I$. As the force of impact is nonzero, ($\approx -19.4N$), not only is the contact unstable causing the robot to bounce on the surface, but also the robot does not contact the surface at the desired location.

Fig. 2: An intuitive example showing the behavior of the proposed control in three different regions. $f(x,\dot{x}) = \begin{bmatrix} -1 & 0 \\ -40 & -25 \end{bmatrix} \dot{x} + \begin{bmatrix} -1 & 0 \\ 0 & -1 \end{bmatrix} (x - x^t)$, where $x^t = [0.1\ \ -0.2]^T$.

where $\mathbf{f}_j(x,\dot{x}) = \dfrac{f(x,\dot{x},t)^T q_j}{f(x,\dot{x},t)^T f(x,\dot{x},t)}$ and ω is defined based on (5) (or its equivalent in Proposition 1) and

$$\frac{\delta_{\dot{x}} - {q_1}^T \dot{x}_0}{e^1 - 1} < \nu \tag{15}$$

Proof: see Appendix D.

$\lambda_1(x,\dot{x})$ defined by (12)-(14) is continuous. The main advantages of the modulation function proposed for the inelastic impact over the elastic one is in its handling of uncertainties in the surface location:

***Proposition** 4:* We assume a planar surface with equation ${q_1}^T x = \eta$, whose orientation is precisely defined through its normal (N) but whose location (η) is imprecise but bounded with a known upper bound $\boldsymbol{\eta}$, i.e. $|\eta| \leq \boldsymbol{\eta} < \rho$. Moreover, for a given initial state $x_0, \dot{x}_0 \in \mathbb{R}^d |\ {q_1}^T \dot{x}_0 < \delta_{\dot{x}} < 0, 0 \leq \boldsymbol{\eta} < {q_1}^T x_0 \leq \rho$, the dynamics of the robot is generated by the nominal DS (1) modulated by (2), where $\lambda_{1j}(x,\dot{x}),\ \forall(j) \in \{1,2,\ldots,d\}$ are defined by (12). Then, the velocity of the robot when it impacts the surface is bounded and satisfies condition (11), if ν and ω are defined as follows:

$$\nu = -\delta_{\dot{x}}, \quad \omega = \frac{\delta_{\dot{x}} - {q_1}^T \dot{x}_0}{{q_1}^T x_0 - \boldsymbol{\eta}} \tag{16}$$

Proof: see Appendix E.

Proposition 4 ensures that the contact is stable and *Objective 1* is satisfied. However, the uncertainty on the location of the surface must remain bounded within a small region. Moreover, the contact location can not be precisely specified.

TABLE I: The details of the systematic assessment. All the positions are with respect to the robot's base. The units are defined in the metric system. $\delta_{\dot{x}} = -0.01ms^{-1}$ and $\rho = 0.2m$. " Contact ", "Leaving/ Stopping" errors are the Euclidean distance between the real and the desired corresponding points. "Pre-contact" and "Pre-transition" velocities are the velocity of the end-effector in the normal direction when entering the *contact* and *transition* regions, respectively.

Experimental set-up 1: Metallic surface and plastic tool		
	Scenario 1	Scenario 2
Initial position	$[-0.5\pm0.2\ \ -0.0\pm0.4\ \ 0.8\pm0.1]$	$[-0.5\pm0.1\ \ -0.0\pm0.3\ \ 0.8\pm0.1]$
Contact Error	0.0 ± 0.03	$0.0\pm2\times10^{-3}$
Leaving/Stopping Error	0.0 ± 0.01	$0.0\pm4\times10^{-3}$
Pre-contact velocity	0.008 ± 0.006	0.007 ± 0.001
Pre-transition velocity	0.24 ± 0.14	0.25 ± 0.13
Experimental set-up 2: Metallic surface and tool		
	Scenario 1	Scenario 2
Initial position	$[-0.5\pm0.1\ \ -0.2\pm0.3\ \ 0.8\pm0.2]$	$[-0.5\pm0.1\ \ -0.0\pm0.3\ \ 0.8\pm0.2]$
Contact Error	0.0 ± 0.02	$0.0\pm\times10^{-3}$
Leaving/Stopping Error	$0.0\pm6\times10^{-3}$	$0.0\pm2\times10^{-3}$
Pre-contact velocity	0.006 ± 0.00	0.006 ± 0.00
Pre-transition velocity	0.29 ± 0.02	0.27 ± 0.04

The performance of the proposed framework is illustrated by a simple intuitive 2-D example in Fig.2, where, in Fig.2a, by using the proposed framework, the robot can stably transit to the contact region. Fig.2b illustrates an unstable contact where the modulation function is disabled by setting $M(x,\dot{x}) = I$. In this case, as contact velocity is very high, the robot bounces on the surface. The source code in C++ is available on-line https://github.com/sinamr66/CoDs_SDK.

IV. Empirical validation

We consider a task of wiping a surface. The performance of the proposed framework is evaluated on a real robotic arm platform, i.e., 7 DOF robotic arm (KUKA IIWA). The robot is controlled at the level of joint positions at a rate of 200 Hz. The output of the DS (1) is converted into the joint state using the damped least squares inverse kinematic solver. The robot is equipped with a 6-axis ATI force-torque sensor which is only used for recording forces and not in the controller. The nominal DS is a second order dynamical system: $f(x,\dot{x}) = -40\dot{x} - \begin{bmatrix} 400 & 0 & 0 \\ 0 & 400 & 0 \\ 4000 & 4000 & 400 \end{bmatrix}(x - x^t)$. These values were chosen such that the robot enters the transition region.

The surface of the fender is approximated by a plane which is calculated by capturing the position of three markers on the surface. The positions are captured by an Optitrack motion capture system. The orientation of the end-effector is constrained to be normal to the contact surface. The impact is assumed inelastic and $\delta_{\dot{x}} = -0.01ms^{-1}$.

The empirical validation is divided into three parts. In the first part, we systematically assess the performance of the controller in executing the two scenarios illustrated in Fig.1a and Fig.1b in a known environment. In the second part, we assess the controller's performance in modulating the robot's motion in a dynamically changing environments. In the third part, the performance of the controller is assessed in an uncertain environment.

1) Systematic assessment: Two experimental set-ups are designed to assess the performance of the system. In the first one, the surface is planar and both surface and the tool are metallic and rigid. In the second one, the surface is a metallic fender and the tool is made from plastic. Both scenarios were repeated 30 times for each set-up where the initial state of the robot is randomly chosen; all the information is summarized in Tab. I. The location of the surface is fixed. The snapshots of the motion execution in both experimental-set-ups are shown in Fig. 3 and Fig. 4. Visual inspection of video and the measured force profiles confirms that, in all the trials, the robot stably makes contact with the surface and accomplishes the tasks. However, the inspection of the measured velocity profiles indicates that in three cases the velocity at impact is higher than $0.01ms^{-1}$. An example of the motion of the robot is illustrated in Fig. 4. As can be seen, the normal velocity of the robot is reduced to $\delta_{\dot{X}}$ in the *transition* region to ensure a stable contact.

As reported in Table I, the overall position errors at x^c, x^l and x^s are very small and they can be considered to be negligible in the wiping scenario. This indicates that even though the surface is not exactly planar in our implementation, our modulation function is capable of accomplishing the desired tasks. These inaccuracies can be attributed to three different causes. i) The main cause of this error is the approximation of the contact surface. In this experiment, we assumed that the contact surface is a plane. However, the fender's surface is bumpy. This results in inaccuracies in the measurement of the distance between the robot and the real surface. ii) The second cause of error is the inverse kinematic [approximation] algorithm. Although, the motion of the robot is not super fast, the IK solver is still unable to generate a very accurate joint-level motion corresponding to the desired end-effector trajectory. The kinematic constraints of the robot are the main reasons for this shortcoming. iii) The third cause of the error is delays in measuring the joint positions and the communication channels. As the robot runs closed-loop, any measuring delays cause inaccuracies in specifying the desired motion of the robot. In spite of these, the overall performance of the task execution is satisfying and the robot was able to wipe the surface successfully in all the trials.

2) Modulation under perturbations: The second assessment is designed to illustrate the capability of the modulation framework in performing Scenario 1 (Fig.1a) under perturbations. While the robot is moving from the initial location, a human operator perturbs either the robot or the surface. Perturbations on the robot are applied to its end effector. Due to the closed-loop implementation of (1), the robot does not stiffly stick to its current state. Hence, one can grab the robot's end-effector and move it around (Fig. 6). As it can be seen in the accompanying video, when the robot is perturbed, the modulation function modifies the motion of the robot such that *Objective 1*, *Objective 2* and *Objective 3*.a are achieved. We then assess the performance of the controller in a dynamically changing environment. Once the robot started moving, the operator changes the fender's position as well as its orientation (Fig.5). Due to the fact that the modulation function is inherently a linear system, it is computationally efficient. Hence, it can instantaneously modify the robot's motion wrt. the current state of the surface.

3) Modulation under uncertainties: In the final experiment, we assess the performance of the controller in an

(a) 0 s. (b) 3.6 s. (c) 5.6 s. (d) 8.27 s. (e) 8.92 s. (f) 9.51 s. (g) 9.8 s. (h) 10.16 s.

Fig. 3: Close-up snapshots of the end-effector motion while performing Scenario 1. Both surface and the tool are metallic and rigid. The robots gets into contact with the surface at (d) and leaves the surface at (g).

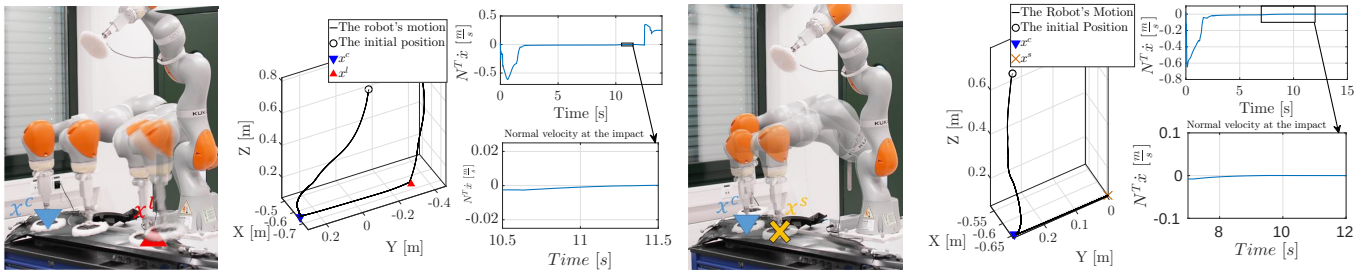

(a) Scenario 1 (b) Scenario 1 (c) Scenario 2 (d) Scenario 2

Fig. 4: In Fig. 4a and Fig. 4c, the location of the surface is precisely measured. In the bottom right figures, the normal velocity of the robot at the impact region is illustrated. $\delta_{\dot{x}} = -0.01ms^{-1}$. The videos are also available on-line at https://youtu.be/fhfBBMH4XVg and https://youtu.be/uHaElQRmofk.

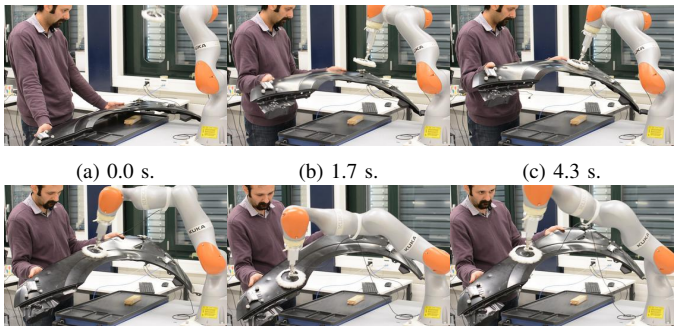

(a) 0.0 s. (b) 1.7 s. (c) 4.3 s.

(d) 8.3 s. (e) 10.2 s. (f) 11.1 s.

Fig. 5: Snapshots of the motion of the robot in a dynamically changing environment. (a) is the initial location. In (c), the robot makes contact with the surface at x^c. In (d), the robots slides on the surface while the surface's orientation is changed. In (e), the robot reaches x^l and, consequently, leaves the surface as depicted in (f).

uncertain environment while performing Scenario 1 (Fig.1a). Uncertainties are modeled as random noise on the location of the surface, where $\boldsymbol{\eta} = 0.15m$. As $\delta_{\dot{x}} = -0.01ms^{-1}$ and ${q_1}^T x_0 = \rho = 0.2$ and ${q_1}^T \dot{x}_{max} = -0.4ms^{-1}$, and based on (16), $\nu = 0.1$ and $\omega = 78$. The experiment was repeated 30 times; see the accompanying video and Table II. In all 30 trials, the impacts were stable. However, as expected, the robot does not exactly make contact with the surface at x^c. Moreover, as a force/tactile sensor was not used, the robot has no way to recognize that a contact occurred. Hence, in 28 out of 30 cases, the robot does not slide on the surface, after the contact, to reach x^l. In the other two cases, η was approximately 0.

TABLE II: The details of the systematic assessment of the controller in an uncertain environment. As $\eta = 0.15$ and $\rho = 0.20$, the effective transition region is $5cm$. Although, the arm does not contact the surface at x^c, the contact is stable and, hence, the robot slides on the surface till it reaches x^c. The contact error is almost constant for $\eta < 0.1$ and it exponentially increases for $0.1 \leq \eta$.

	Scenario 1
Initial position	$\begin{bmatrix} -0.5 \pm 0.1 \\ -0.1 \pm 0.3 \\ 0.8 \pm 0.2 \end{bmatrix}$
η	0.06 ± 0.04
Contact error	0.0764 ± 0.13
Pre-contact velocity	0.006 ± 0.005
Pre-transition velocity	0.13 ± 0.013

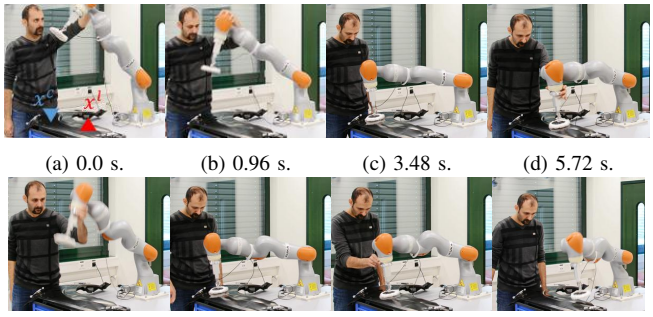

(a) 0.0 s. (b) 0.96 s. (c) 3.48 s. (d) 5.72 s.

(e) 6.47 s. (f) 14.81 s. (g) 16.32 s. (h) 18.18 s.

Fig. 6: Snapshots of the motion of the robot while performing Scenario 1 under perturbations. As $\eta = 15$ and $\rho = 20$, the effective transition region is $5cm$. Due to the closed loop implementation of (1), the robot complies with the human operator in all directions.

V. Summary and Discussion

In this paper, we propose a controller for locally modulating a motion of the robot during non-contact/contact transitions. Using/employing this approach, the robot reduces its velocity to a certain threshold before entering into contact with the surface such that the post-contact velocity becomes zero; i.e. the impact is stable and the robot does not bounce on the surface. Furthermore, by modulating the motion of the robot in the tangential directions, we showed that the contact location can be specified. Moreover, while the robot slides on the surface, it can either leave or stop on the surface at the desired departure or stop points, respectively.

Throughout the proofs, we assume that x^* is a fixed target. However, in two cases it is not constant. In the first case, x^* is changed wrt. the state of the robot in Proposition 2 and 3. This does not actually affect the performance of the system for two reasons as changing x^* based on (8) or (9) does not affect the motion of the robot in the normal direction. Hence, the switch between $0 < N^T x$ and $N^T x = 0$ happens only once. In the second case, x^* changes while the surface is

perturbed. In this case, as the modulation function is very fast to compute and its convergence rate is faster than the update rate, it can properly react, in real-time, to the perturbations as presented in Section IV-.2.

In Section IV, the modulated DS is implemented in closed-loop as the low-level controller of IIWAs fully compensates for the robot's dynamics and it is safe to assume that the measured position is equal to the commanded position. However, this assumption might not be true in other robotic platforms. In these cases, in order to ensure the stability of contact, one needs to study the behavior of the modulated-DS while considering the robot's controller and dynamics.

As the sole information about the surface is its location, any inaccuracies in the position measurements deteriorate the performance of the controller. To address this, we present Proposition 4 to improve the robustness of the system in face of uncertainties in the location of the surface. This, however, fails in identifying the true location of the surface once the robot makes contact with the surface. By integrating our modulation framework and force control architectures, one can use the force-feedback information not only for identifying the true location of the surface, but also for controlling the contact force while the robot is on the surface.

Even though, the performance of the system is successfully evaluated on a bumpy surface, in this paper, the contact surface is assumed planar. We are currently working on generalizing the framework such that general shaped surfaces can also be considered. Furthermore, in this work, we do not control for the forces and hence could not compensate for strong frictional forces. To address this, ongoing work is oriented towards unifying force control frameworks with the proposed motion generator such that one can precisely control for the interaction of (both normal and frictional) forces while the robot slides on the surface.

ACKNOWLEDGEMENTS

This work was supported by the EU project Cogimon H2020 ICT 23 2014. Authors thank Nadia Figueroa, Yonadav Shavit and Andrew Sutcliffe for their help.

APPENDIX

A. Proof of Theorem 1

By definition, Q is an orthonormal matrix; i.e $QQ^T = I,\ Q^T = Q^{-1}$. Moreover, as $q_i\ \forall i \in \{1,\dots,d\}$ form an orthonormal basis in $\mathbb{R}^d$, $\forall w \in \mathbb{R}^d$:$w = \sum_{i=1}^{d} q_i {q_i}^T w$. Substituting (4) and (2) into (1) and multiplying both sides of the resultant equation by q_1^T yields:

$$
\begin{aligned}
&{q_1}^T \ddot{x} = {q_1}^T Q\Lambda Q^{-1} f(.) = \sum_{j=1}^{d} \lambda_{1j}(x,\dot{x}) q_j^T f(.) = \sum_{j=1}^{d} \frac{-2\omega N^T \dot{x} - \omega^2 N^T x}{f(.)^T f(x,\dot{x},t)} f(.)^T q_j q_j^T f(.) \\
&= \frac{-2\omega N^T \dot{x} - \omega^2 N^T x}{f(.)^T f(.)} f(.)^T \sum_{j=1}^{d} q_j q_j^T f(.) = \left(-2\omega N^T \dot{x} - \omega^2 N^T x\right) \frac{f(.)^T f(x,\dot{x},t)}{f(.)^T f(.)} \\
&= -2\omega N^T \dot{x} - \omega^2 N^T x
\end{aligned}
\tag{17}
$$

Which is a critically-damped second order linear differential equation where ω defines the natural frequency of this system. The solution of (17) for a given initial state $\{x_0, \dot{x}_0\}$ is:

$$
{q_1}^T x = e^{-t\omega}({q_1}^T x_0 + ({q_1}^T x_0 \omega + {q_1}^T \dot{x}_0) t) \tag{18}
$$

Based on (5), as $\frac{|{q_1}^T \dot{x}_0|}{{q_1}^T x_0} \leq \omega$ and $0 < {q_1}^T x_0$, $0 \leq {q_1}^T x_0 \omega + {q_1}^T \dot{x}_0$. Hence, (18) is zero only when t tends to infinity; i.e. $\lim_{t \to +\infty} {q_1}^T x = 0$. Moreover, the time derivative of (18) at $t = +\infty$ is zero; i.e. $\lim_{t \to +\infty} {q_1}^T \dot{x} = \lim_{t \to +\infty} e^{-t\omega}({q_1}^T \dot{x}_0 - ({q_1}^T x_0 \omega + {q_1}^T \dot{x}_0)\omega t) = 0$. Hence, the motion generated by 1 and 2 with respect to (4) and (5), enters the contact surface with zero normal velocity. Hence, *Objective 1* is satisfied.

Similar to (17), substituting (6) and (2) into (1) and multiplying both sides of the resultant equation by $q_i,\ \forall i \in \{2,\dots,d\}$ yields:

$$
{q_i}^T \ddot{x} = {q_i}^T Q\Lambda Q^{-1} f(.) = \sum_{j=1}^{d} \lambda_{ij}(x,\dot{x}) {q_j}^T f(.) = -2\omega {q_i}^T \dot{x} - \omega^2 {q_i}^T (x - x^*) \tag{19}
$$

Which is a second order linear differential equation. Similar to (18), the solution of (19) for a given initial state $\{x_0, \dot{x}_0\}$ converges to ${q_i}^T x^*$ when t tends to infinity; i.e. $\lim_{t \to +\infty} \|{q_i}^T x - {q_i}^T x^*\| = 0$. Where, in this theorem, $x^* = x^c$. As this holds $\forall i \in \{2,\dots,d\}$ and the rate of change of (17) and (19) are the same, the motion reaches x^c when $t = +\infty$, the dynamical system (1) and (2) with respect to (5) and (6) contacts the surface at x^c; i.e. *Objective 2* is satisfied. ■

B. Proof of Proposition 1

As the modulation function is activated once the robot enters the transition region, $\rho = {q_1}^T x_0$. Substituting (4) and (2) into (1) with $\omega = \frac{|{q_1}^T \dot{x}_0|}{\rho}$ and multiplying both sides of the resultant equation by ${q_1}^T$ yields:

$$
\begin{aligned}
&{q_1}^T \ddot{x}_{max} = -2\omega {q_1}^T \dot{x}_0 - \omega^2 {q_1}^T x_0 = -2\omega {q_1}^T \dot{x}_0 - \omega^2 \rho = -2\frac{|{q_1}^T \dot{x}_0|}{\rho} {q_1}^T \dot{x}_0 - (\frac{{q_1}^T \dot{x}_0}{\rho})^2 \rho \Rightarrow \\
&\rho = \frac{-2|{q_1}^T \dot{x}_0| {q_1}^T \dot{x}_0 - ({q_1}^T \dot{x}_0)^2}{{q_1}^T \ddot{x}_{max}}
\end{aligned}
\tag{20}
$$

To be safe, we take the upper bound of (20), i.e. :$\rho = \frac{3({q_1}^T \dot{x}_{max})^2}{|{q_1}^T \ddot{x}_{max}|}$. Substituting this into $\omega = \frac{|{q_1}^T \dot{x}_0|}{\rho}$ yields:$\omega = |\frac{{q_1}^T \ddot{x}_{max}}{3{q_1}^T \dot{x}_{max}}|$. ■

C. Proof of Proposition 3

x^I is located in the middle of x^c and $2x^I - x^c$.Once the robot is in contact with the surface (${q_1}^T x = 0$), as the motion generated by (6) moves on a straight line towards $x^* = 2x^I - x^c$, it passes x^I. Moreover, the modulation part of (10) is less than ρ for all the points between x^c and x^I as $\forall \theta \in [0,1)$ and $x = x^c + \theta(x^I - x^c)$

$$
\begin{aligned}
&\left(\rho - (x^I - x^c)^T (x^I - x)\right) e^{-(x^I - x)^T \Sigma^{-1} (x^I - x)} = \\
&\left(\rho - (x^I - x^c)^T (x^I - x^c - \theta(x^I - x^c))\right) e^{-(1-\theta)^2 (x^I - x^c)^T \Sigma^{-1} (x^I - x^c)} = \\
&\left(\rho \underbrace{-(1-\theta)(x^I - x^c)^T (x^I - x^c)}_{0<}\right) \underbrace{e^{-(1-\theta)^2 (x^I - x^c)^T \Sigma^{-1} (x^I - x^c)}}_{<1} < \rho
\end{aligned}
\tag{21}
$$

However, if $\lim_{\theta \to 1^+}$, the modulation part of (10) is greater than ρ. Hence, once the robot passes x^I, the modulation function is deactivated based on (3) and the nominal dynamical system leaves the surface to converge to x^I. However, it is important to note that if Σ is very small, even thought it leaves the surface at x^I, the motion might not converge to x^I. ■

D. Proof of Theorem 2

Substituting (12)-(14) and (2) into (1) and multiplying both sides of the resultant equation by q_1^T yields:

$$
{q_1}^T \ddot{x} = \begin{cases}
-\omega\left({q_1}^T \dot{x} - (\delta_{\dot{x}} + \nu)\right) & {q_1}^T \dot{x} < \delta_{\dot{x}} \qquad (22) \\
\frac{\omega^2 {q_1}^T x + \nu\omega}{\delta_{\dot{x}}} {q_1}^T \dot{x} - \omega^2 {q_1}^T x & \delta_{\dot{x}} \leq {q_1}^T \dot{x} \leq 0 \qquad (23) \\
-2\omega N^T \dot{x} - \omega^2 N^T x & 0 < {q_1}^T \dot{x} \qquad (24)
\end{cases}
$$

${q_1}^T \ddot{x}$ defined by (22)-(24) is continuous. Based on ${q_1}^T \dot{x}_0$, the proof of Theorem 2 needs to be done in three different velocity regions. In the **third** region, $0 < {q_1}^T \dot{x}_0$. Hence, based on (24): ${q_1}^T \ddot{x} = -2\omega {q_1}^T \dot{x} - \omega^2 {q_1}^T x$, which is equal to (17). Hence, as shown in Appendix A, as long as $\frac{|{q_1}^T \dot{x}_0|}{{q_1}^T x_0} \leq \omega$, the motion reaches the surface with zero velocity. Hence, *Objective 1* is satisfied.

In the **second** region, $\delta_{\dot{x}} \leq {q_1}^T \dot{x} \leq 0$. Hence, based on (23), ${q_1}^T \ddot{x} = \frac{\omega^2 {q_1}^T x + \nu\omega}{\delta_{\dot{x}}} {q_1}^T \dot{x} - \omega^2 {q_1}^T x$. The aforementioned DS yields that if ${q_1}^T \dot{x} = \delta_{\dot{x}}$, ${q_1}^T \ddot{x} = \omega\nu$, where, based on (15), $0 < \omega\nu$. This means that once ${q_1}^T \dot{x}$ enters this region, it does not cross the velocity boundary at $\delta_{\dot{x}}$; i.e. it does not get less than $\delta_{\dot{x}}$. Moreover, while the robot is above the surface (i.e. $0 < {q_1}^T x$) and ${q_1}^T \dot{x} = 0$, the normal acceleration is negative; i.e. ${q_1}^T \ddot{x} \leq 0$. Hence, the robot's normal velocity can not get higher than zero. To sum up, if ${q_1}^T \dot{x}$ is in this region, the robot moves towards the contact surface with the velocity between 0 and $\delta_{\dot{x}}$. Hence, *Objective 1* is satisfied.

In the **first** region, ${q_1}^T \dot{x}_0 < \delta_{\dot{x}}$. Hence, based on (22), ${q_1}^T \ddot{x} = -\omega({q_1}^T \dot{x} - (\delta_{\dot{x}} + \nu))$. The solution of the aforementioned dynamic for a given initial state $\{x_0, \dot{x}_0\}$ is given by:

$$
{q_1}^T x(t) = \frac{(\nu + \delta_{\dot{x}} - {q_1}^T \dot{x}_0) e^{-\omega^{-1} t} + \omega({q_1}^T x_0 + \nu t + \delta_{\dot{x}} t) + (\nu + \delta_{\dot{x}}) t + {q_1}^T \dot{x}_0}{\omega}
$$

(25a)

$$q_1{}^T\dot{x}(t) = (q_1{}^T\dot{x}_0 - \nu - \delta_{\dot{x}})e^{-\omega t} + \delta_{\dot{x}} + \nu \tag{25b}$$

Both (25a) and (25b) are monotonic profiles; i.e. if $0 < q_1{}^T x_0$ and $q_1{}^T\dot{x}_0 < \delta_{\dot{x}}$, (25a) is monotonically decreasing and (25b) is monotonically increasing. Hence, based on (25b), $q_1{}^T\dot{x}(t^*) = \delta_{\dot{x}}$ at $t^* = -ln(\frac{\nu}{\nu+\delta_{\dot{x}}-q_1{}^T\dot{x}_0})\omega^{-1}$. Given $q_1{}^T\dot{x}_0 < \delta_{\dot{x}}$, substituting (5), (15) and t^* into (25a) yields

$$\begin{aligned} q_1{}^T x(t^*) &= (\delta_{\dot{x}} + \nu)(-\omega^{-1}\ln(\frac{\nu}{\nu+\delta_{\dot{x}}-q_1{}^T\dot{x}_0})) + (q_1{}^T\dot{x}_0 - \delta_{\dot{x}})\omega^{-1} + q_1{}^T x_0 \\ &= (-(\delta_{\dot{x}} + \nu)\ln(\frac{\nu}{\nu+\delta_{\dot{x}}-q_1{}^T\dot{x}_0}) - \delta_{\dot{x}} + q_1{}^T\dot{x}_0)\omega^{-1} + q_1{}^T x_0 \end{aligned} \tag{26}$$

As $-\frac{q_1{}^T\dot{x}_0}{q_1{}^T x_0} \leq \omega$, $q_1{}^T x(t^*)$ defined by (26) is bounded:

$$\begin{aligned} &\frac{q_1{}^T x_0 \delta_{\dot{x}}}{q_1{}^T\dot{x}_0}\left(\ln\left(\frac{\nu}{\nu+\delta_{\dot{x}}-q_1{}^T\dot{x}_0}\right)+1\right) + \frac{q_1{}^T x_0\,\nu}{q_1{}^T\dot{x}_0}\ln\left(\frac{\nu}{\nu+\delta_{\dot{x}}-q_1{}^T\dot{x}_0}\right) \\ &\leq q_1{}^T x(t^*) < q_1{}^T x_0 \end{aligned} \tag{27}$$

By defining $0 < \frac{\delta_{\dot{x}}-q_1{}^T\dot{x}_0}{e^1-1} < \nu$, the lower bound of (27) will be positive:

$$0 < \underbrace{\frac{q_1{}^T x_0 \delta_{\dot{x}}}{q_1{}^T\dot{x}_0}}_{0<}\underbrace{\left(\ln\left(\frac{\nu}{\nu+\delta_{\dot{x}}-q_1{}^T\dot{x}_0}\right)+1\right)}_{0<} + \underbrace{\frac{q_1{}^T x_0\,\nu}{q_1{}^T\dot{x}_0}}_{<0}\underbrace{\ln\left(\frac{\nu}{\nu+\delta_{\dot{x}}-q_1{}^T\dot{x}_0}\right)}_{<0} \tag{28}$$

Hence, the robot's normal velocity is $\delta_{\dot{x}}$ before it gets into the contact. Moreover, as $0 < q_1{}^T\ddot{x}$ if $q_1{}^T\dot{x} = \delta_{\dot{x}}$, the robot moves toward the contact surface with $\delta_{\dot{x}} \leq q_1{}^T\dot{x}$. To sum up, in all three regions, the proposed modulation function regulates the normal velocity of the robot such that it satisfies (11) before the robot gets into the contact with the surface. ■

E. Proof of Proposition 4

To satisfy (11) when the location of the surface is uncertain, we need to study the worse scenario; namely when $\eta = \boldsymbol{\eta}$. In this case, to achieve *Objective 1*, the robot's normal velocity must be $\delta_{\dot{x}}$ at $q_1{}^T x = \boldsymbol{\eta}$. Hence, (26) should lower bounded by $\boldsymbol{\eta}$:

$$(-(\delta_{\dot{x}} + \nu)\ln(\frac{\nu}{\nu+\delta_{\dot{x}}-q_1{}^T\dot{x}_0}) - \delta_{\dot{x}} + q_1{}^T\dot{x}_0)\omega^{-1} + q_1{}^T x_0 = \boldsymbol{\eta} \tag{29}$$

Moreover, Theorem 2 requires that: $0 < \nu \leq -\delta_{\dot{x}}$, $0 < \omega$. Equation (29) with respect to $0 < \nu \leq -\delta_{\dot{x}}, 0 < \omega$ does not have a unique solution. Hence, one can use numerical solvers to minimize ω with respect to (29) and $0 < \nu \leq -\delta_{\dot{x}}$, $0 < \omega$. However, as $\boldsymbol{\eta} < q_1{}^T x_0$ and $q_1{}^T\dot{x}_0 < \delta_{\dot{x}}$, one can set $\nu = -\delta_{\dot{x}}$ and $\omega = \frac{\delta_{\dot{x}}-q_1{}^T\dot{x}_0}{q_1{}^T x_0 - \boldsymbol{\eta}}$. This, based on our experience, results in an acceptable performance. To conclude, by defining (16), $q_1{}^T\dot{x}(t) = \delta_{\dot{x}}$ at $q_1{}^T x(t) = \boldsymbol{\eta}$. Hence, $\forall\eta \in [-\boldsymbol{\eta}, \boldsymbol{\eta}]$, based on (13), the robot's velocity at the contact is $\delta_{\dot{x}} \leq q_1{}^T\dot{x}$; i.e. (11) is satisfied. ■

REFERENCES

[1] A. M. Kabir, K. N. Kaipa, J. Marvel, and S. K. Gupta, "Automated planning for robotic cleaning using multiple setups and oscillatory tool motions," *IEEE Transactions on Automation Science and Engineering*, 2017.

[2] P. R. Pagilla and B. Yu, "Robotic surface finishing processes: modeling, control, and experiments," *Transactions-American Society of Mechanical Engineers Journal of Dynamic Systems Measurement and Control*, vol. 123, no. 1, pp. 93–102, 2001.

[3] D. Leidner, A. Dietrich, M. Beetz, and A. Albu-Schäffer, "Knowledge-enabled parameterization of whole-body control strategies for compliant service robots," *Autonomous Robots*, vol. 40, no. 3, pp. 519–536, Mar 2016.

[4] C. Schindlbeck and S. Haddadin, "Unified passivity-based cartesian force/impedance control for rigid and flexible joint robots via task-energy tanks," in *2015 IEEE International Conference on Robotics and Automation (ICRA)*, May 2015, pp. 440–447.

[5] N. Figueroa, A. L. Pais Ureche, and A. Billard, "Learning complex sequential tasks from demonstration: A pizza dough rolling case study," in *ACM/IEEE Intern. Conf. on Human Robot Interaction*. IEEE Press, 2016, pp. 611–612.

[6] Y.-B. Jia, M. T. Mason, and M. A. Erdmann, "Multiple impacts: A state transition diagram approach," *The Intern. Journal of Robotics Research*, vol. 32, no. 1, pp. 84–114, 2013.

[7] P. R. Pagilla and B. Yu, "A stable transition controller for constrained robots," *IEEE/ASME Transactions on Mechatronics*, vol. 6, no. 1, pp. 65–74, Mar 2001.

[8] J. K. Mills and D. M. Lokhorst, "Stability and control of robotic manipulators during contact/noncontact task transition," *IEEE Transactions on Robotics and Automation*, vol. 9, no. 3, pp. 335–345, 1993.

[9] J. K. Mills, "Manipulator transition to and from contact tasks: A discontinuous control approach," in *IEEE Intern. Conf. on Robotics and Automation*. IEEE, 1990, pp. 440–446.

[10] T.-J. Tarn, Y. Wu, N. Xi, and A. Isidori, "Force regulation and contact transition control," *IEEE Control Systems*, vol. 16, no. 1, pp. 32–40, 1996.

[11] D. J. F. Heck, A. Saccon, N. van de Wouw, and H. Nijmeijer, "Switched position-force tracking control of a manipulator interacting with a stiff environment," in *2015 American Control Conf. (ACC)*, July 2015, pp. 4832–4837.

[12] M. Tomizuka, "Contact transition control of nonlinear mechanical systems subject to a unilateral constraint," *Journal of dynamic systems, measurement, and control*, vol. 119, p. 749, 1997.

[13] K. Youcef-Toumi and D. A. Gutz, "Impact and force control," in *IEEE Intern. Conf. on Robotics and Automation*. IEEE, 1989, pp. 410–416.

[14] L. Roveda, G. Pallucca, N. Pedrocchi, F. Braghin, and L. M. Tosatti, "Iterative learning procedure with reinforcement for high-accuracy force tracking in robotized tasks," *IEEE Transactions on Industrial Informatics*, vol. PP, no. 99, pp. 1–1, 2017.

[15] L. Roveda, N. Iannacci, F. Vicentini, N. Pedrocchi, F. Braghin, and L. M. Tosatti, "Optimal impedance force-tracking control design with impact formulation for interaction tasks," *IEEE Robotics and Automation Letters*, vol. 1, no. 1, pp. 130–136, Jan 2016.

[16] E. Lee, J. Park, K. A. Loparo, C. B. Schrader, and P. H. Chang, "Bang-bang impact control using hybrid impedance/time-delay control," *IEEE/ASME Transactions on Mechatronics*, vol. 8, no. 2, pp. 272–277, June 2003.

[17] M. Jin, S. H. Kang, P. H. Chang, and E. Lee, "Nonlinear bang-bang impact control: A seamless control in all contact modes," in *Proceedings of the 2005 IEEE Intern. Conf. on Robotics and Automation*, April 2005, pp. 557–564.

[18] C. Liang, S. Bhasin, K. Dupree, and W. E. Dixon, "A force limiting adaptive controller for a robotic system undergoing a non-contact to contact transition," in *2007 46th IEEE Conf. on Decision and Control*, Dec 2007, pp. 3555–3560.

[19] A. Tornambe, "Modeling and control of impact in mechanical systems: theory and experimental results," *IEEE Transactions on Automatic Control*, vol. 44, no. 2, pp. 294–309, Feb 1999.

[20] K. Dupree, C. H. Liang, G. Hu, and W. E. Dixon, "Adaptive Lyapunov-based control of a robot and mass-spring system undergoing an impact collision," *IEEE Transactions on Systems, Man, and Cybernetics, Part B (Cybernetics)*, vol. 38, no. 4, pp. 1050–1061, Aug 2008.

[21] B. Brogliato, S. I. Niculescu, and P. Orhant, "On the control of finite-dimensional mechanical systems with unilateral constraints," *IEEE Transactions on Automatic Control*, vol. 42, no. 2, pp. 200–215, Feb 1997.

[22] F. Ferraguti, C. Secchi, and C. Fantuzzi, "A tank-based approach to impedance control with variable stiffness." in *IEEE Intern. Conf. on Control Automation (ICRA*, 2013, pp. 4948–4953.

[23] M. Martino and M. E. Broucke, "A reach control approach to bumpless transfer of robotic manipulators," in *53rd IEEE Conf. on Decision and Control*, Dec 2014, pp. 25–30.

[24] S. S. M. Salehian, M. Khoramshahi, and A. Billard, "A dynamical system approach for softly catching a flying object: Theory and experiment," *IEEE Transactions on Robotics*, vol. 32, no. 2, pp. 462–471, April 2016.

[25] S. S. M. Salehian, N. Figueroa, and A. Billard, "Coordinated multi-arm motion planning: Reaching for moving objects in the face of uncertainty," in *Proceedings of Robotics: Science and Systems*, AnnArbor, Michigan, June 2016.

[26] S.-M. Khansari-Zadeh and A. Billard, "A dynamical system approach to realtime obstacle avoidance," *Autonomous Robots*, vol. 32, pp. 433–454, 2012, 10.1007/s10514-012-9287-y.

[27] K. Kronander, M. Khansari, and A. Billard, "Incremental motion learning with locally modulated dynamical systems," *Robotics and Autonomous Systems*, vol. 70, pp. 52 – 62, 2015.

[28] S. S. M. Salehian, N. Figueroa, and A. Billard, "A unified framework for coordinated multi-arm motion planning," *The International Journal of Robotics Research*, 2018.

[29] O. Khatib, "Real-time obstacle avoidance for manipulators and mobile robots," *The Intern. journal of robotics research*, vol. 5, no. 1, pp. 90–98, 1986.